

# Relationship Between Vickers Hardness and Fatigue Strength

A. Hirano<sup>1</sup>, M. Sakane<sup>2</sup> and N. Hamada<sup>3</sup>

<sup>1</sup> Department of Automotive Engineering, Junior College of Osaka Sangyo University,  
Osaka, 574-8530, Japan

<sup>2</sup> Department of Mechanical Engineering, Faculty of Science and Engineering, Ritsumeikan University  
Shiga, 525-8577, Japan

<sup>3</sup> Department of Mechanical Engineering, Hiroshima Kokusai Gakuin University  
Hiroshima, 739-0321, Japan

## Abstract

This paper describes the relationship between Vickers hardness and elastic-plastic material constants by using finite element analyses. Finite element analyses for Vickers hardness were carried out for studying the effects of friction and elastic-plastic material constants on the hardness. A new equation for predicting Vickers hardness was proposed as a function of yield stress and strain hardening coefficient and exponent. The fatigue limit and threshold of stress intensity factor were discussed in relation to the elastic-plastic material constants based on the proposed equation.

## 1 Introduction

Hardness testing has been most frequently used material testing and has been understood as a testing to measure the resistance to compressive permanent deformation (Taber [1]). Hardness was investigated systematically in experiments using different materials (Yoshizawa[2]). However, inelastic material constants have been considered to have a close connection with hardness but a quantitative relationship between the constants and hardness has not been well understood.

Recent progress of contact finite element (FE) analyses enabled the numerical analysis of hardness (Karl et al. [3], Talijat et al. [4], Wang et al. [5] and Murakami et al. [6]). FE analyses have the advantage of examining the effect of an inelastic material constant on the hardness keeping the other material constants fixed.

The authors studied the quantitative relationship between the hardness and elastic-plastic material constants using FE analyses for Brinell (Hamada et al. [7]), and Rockwell A (Hamada et al. [8]), B (Hamada et al. [9]) and C (Hirano et al. [10]) scale hardnesses. In these studies, the quantitative relationships between the hardness and elastic-plastic material constants that characterize the inelastic deformation were proposed.

This paper studies the relationship between Vickers hardness (HV) and the elastic-plastic material constants by using FE analyses. Finite element contact analyses were carried out for various yield stresses, strain hardening coefficients and exponents. Based on the quantitative relationship between HV and these material constants, an equation for predicting the hardness from the material constants will be proposed. The accuracy of the equation will be discussed by comparing the hardness between the prediction, FE analysis and experimental results. The influence of the material constants on fatigue limit and threshold of stress intensity factor will be discussed based on the derived equation.

## 2. Finite Element Model

Figure 1 shows FE meshes used in this study to simulate Vickers hardness. A quarter part of a whole model was meshed from the symmetry of the model. The indenter was composed of steel holder and diamond tip with a flank angle of 136 degrees. The numbers of nodes and elements of the mesh are 5353 and 4325, respectively.

MARC K7 was used as a FE code and MENTAT as a pre- and post-processor. True stress-logarithmic strain relationships were used in the FE analysis with the large deformation, update and finite strain options. Contact was judged when the indenter approached to the specimen in the distance less than  $1.0 \times 10^{-5}$  mm.

This study assumed a power law-type inelastic constitutive equation shown below,

$$\varepsilon_p = \left( \frac{\sigma - \sigma_y}{A} \right)^{\frac{1}{n}} \quad (1)$$

where  $\varepsilon_p$ ,  $\sigma$ ,  $\sigma_y$ ,  $A$ , and  $n$  are plastic strain, flow stress, yield stress and strain hardening coefficient and exponent, respectively. In FE analyses,

the load applied to an indenter was increased to the maximum value of 490 N and was decreased to zero to simulate Vickers hardness testing as defined in JIS and ISO standards.

## 3. Analytical Results and Discussion

### 3.1 Comparison of Vickers hardness between FE analysis and experiment

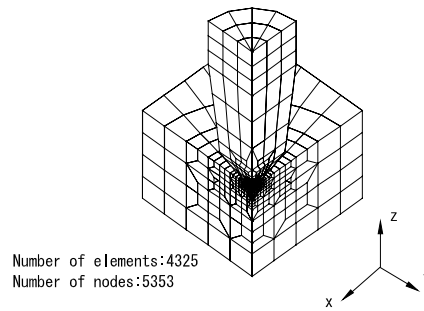


Fig.1 FE models used for FE analyses.

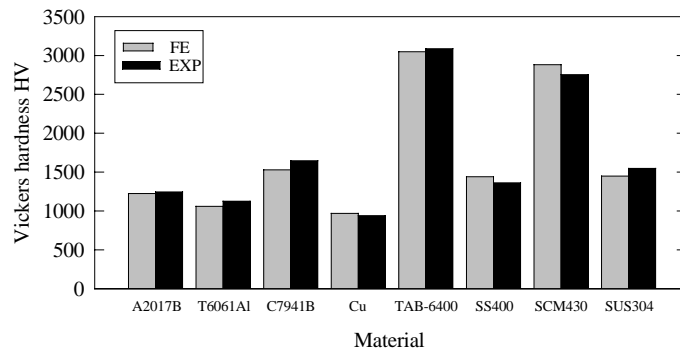


Fig.2 Comparison of Vickers hardness between the FE analysis and experiment for eight materials.

Vickers hardness was calculated from the diagonal distance ( $d$ ), after complete unloading using Eq.(2), where  $F$  is the maximum applied load.

$$HV = 0.189 \times \frac{F}{d^2} \quad (2)$$

Figure 2 compares Vickers hardness between the FE analysis and experiment for the eight materials shown in the figure. The difference of the hardness between the FE analysis and experiment is small so that the FE analyses used in this study accurately simulate the Vickers hardness.

### 3.2 Relationship between Vickers hardness and inelastic material constants

Figures 3 shows the relationship between Vickers hardness and strain hardening coefficient for the material constants shown in the figure. HV is equated with strain hardening coefficient as,

$$HV = \alpha A + \beta \quad (3)$$

where  $\alpha$  and  $\beta$  are the gradient and intercept of the line in the figure. Since  $\alpha$  in Eq.(3) is a function of  $A$  and  $n$ , Fig.4 shows the relationship between  $\alpha$  and  $n$  for various  $A$ 's. The ordinate in Fig.4 is modified with  $A$  to obtain a unique relationship against  $n$ .

The line in the figure is expressed by,

$$\alpha = 4.499n^2 - 5.886n + (-1.810 \times 10^{-4} A + 2.525) \quad (4)$$

Eq.(3) is expressed as a function of  $\sigma_y$  independent of  $n$  as,

$$\beta = 2.701\sigma_y + 123 \quad (5)$$

Substitution Eqs.(4) and (5) into Eq.(3) gives the relationship between the Vickers hardness and the inelastic material constants as,

$$HV_{Pre} = (4.499n^2 - 5.886n + (-1.81 \times 10^{-4} A + 2.525))A + 2.701\sigma_y + 123 \quad (6)$$

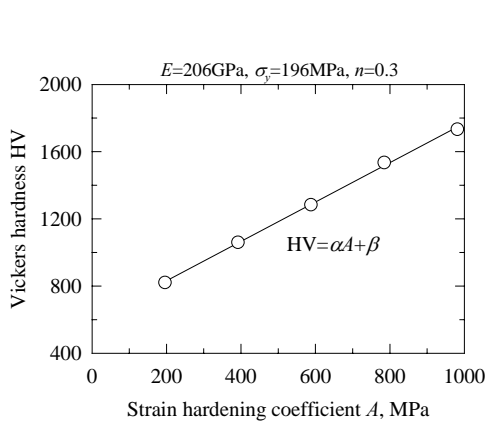


Fig.3 Variation of Vickers hardness with strain hardening coefficient.

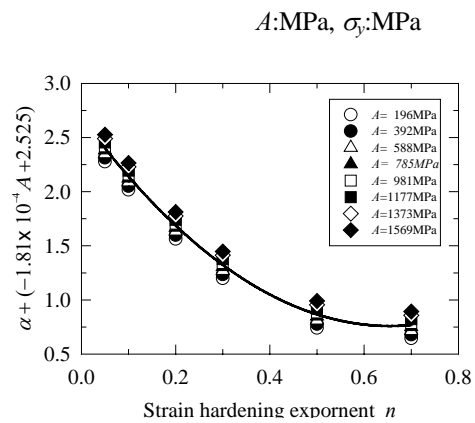


Fig.4 Relationship between  $\alpha$  and strain hardening exponent.

Figure 5 compares the Vickers hardnesses predicted by Eq.(6) with the FE results. Also, the hardnesses of the eight materials obtained in experiments are dotted in the figure of which the predicted values were calculated using Eq.(6) from their material constants. All the hardnesses predicted agree well with the FE and experimental results within a small scatter. Equation (6) also indicates that how yield stress and strain hardening coefficient and exponent influence HV value quantitatively.

### 3.3 Relationship between threshold of stress intensity factor ( $\Delta K_{th}$ ), fatigue limit ( $\sigma_w$ ) and Vickers hardness

The relationship between  $\sigma_w$ ,  $\Delta K_{th}$  and the inelastic material constants are expressed by the following equations for low hardness and high hardness steels (Murakami et al., [11]).

Low hardness steels ( $HV \leq 3923\text{MPa}$ )

$$\sigma_w \cong 1.6HV \pm 0.1HV \quad (7)$$

High hardness steels ( $HV \geq 4900\text{MPa}$ )

$$\sigma_w \cong \frac{1.43(HV + 120)}{\sqrt{(area)s}^{\frac{1}{6}}} \quad (8)$$

$$\sigma_w \cong \frac{1.56(HV + 120)}{\sqrt{(area)i}^{\frac{1}{6}}} \quad (9)$$

$$\Delta K_{th} \cong 3.3 \times 10^{-3} (HV + 120) \sqrt{(area)s}^{\frac{1}{3}} \quad (10)$$

$$\Delta K_{th} \cong 2.77 \times 10^{-3} (HV + 120) \sqrt{(area)i}^{\frac{1}{3}} \quad (11)$$

where the  $\sqrt{(area)s}$  and  $\sqrt{(area)i}$  are the area of inclusion at near specimen surface and in a specimen, respectively.

Figures 6 represents the influence of yield stress  $\sigma_y$  on  $\sigma_w$  calculated by Eq.(7) for low hardness steels. Dotted lines cover a range of  $\pm 0.1HV$  calculated by Eq.(7). The fatigue limit linearly increases with increasing of  $\sigma_y$  as shown in the figure. This result clearly indicates that the fatigue limit of low hardness steels mainly depends on yield stress, whereas  $A$  and  $n$  have a little influence on  $\sigma_w$ , which is not graphically presented here.

Figures 7(a), (b) and (c) show the influence of the  $\sigma_y$ ,  $A$ , and  $n$  on fatigue limit for high hardness

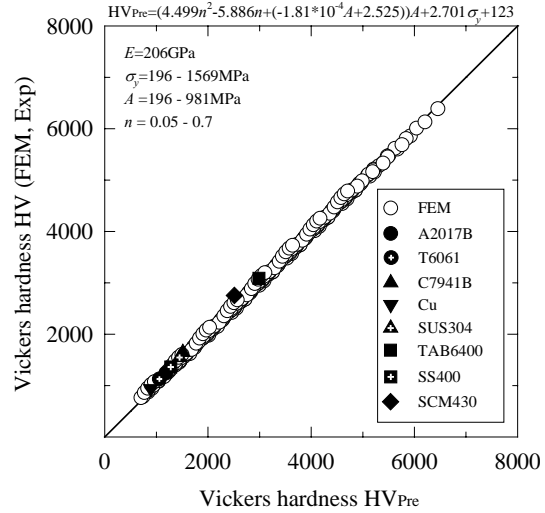


Fig.5 Comparison between the hardness predicted by Eq.(6) and the experimental and FE results.

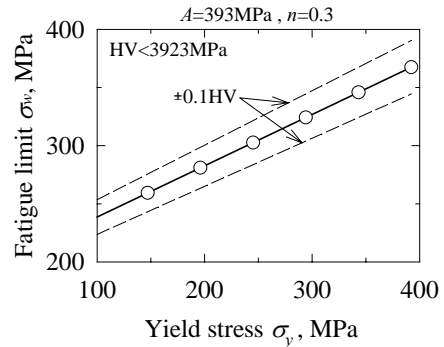


Fig.6 Influence of material constants on fatigue limit for low hardness steels.

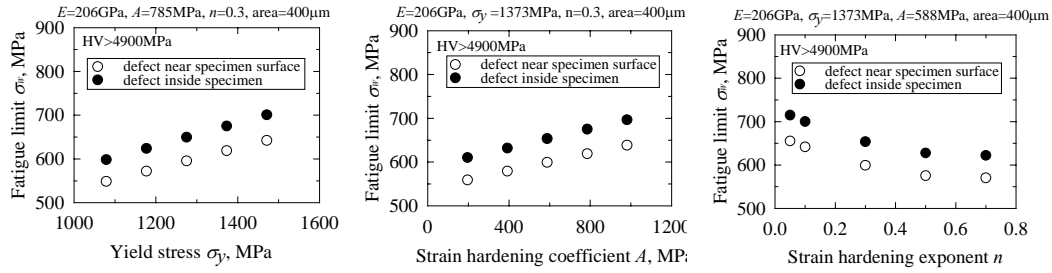


Fig.7 Influence of the material constants on the fatigue limit for high hardness steels.

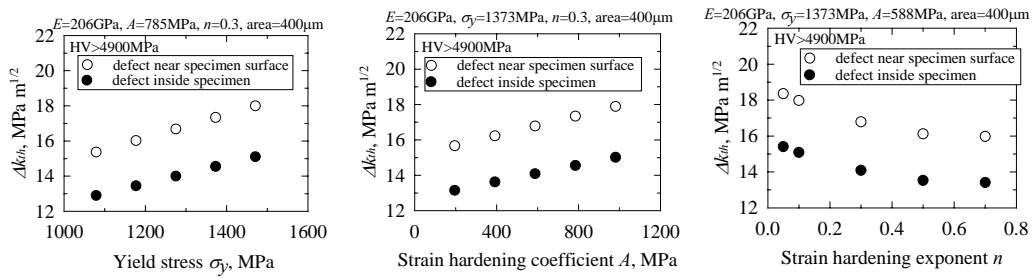


Fig.8 Influence of material constants on the threshold of stress intensity factor for high hardness steels.

steels calculated by Eqs.(8) and (9). Open circles in the figures show the fatigue limit with a defect near in specimen surface and solid circles that with a defect in a specimen. The fatigue limit linearly increases with increasing  $\sigma_y$  and  $A$ , but it decreases with increasing  $n$  for both types of defects. In all the cases shown Figs.7(a), (b) and (c), the defect near specimen surface is more detrimental to the fatigue limit than that inside specimen. Comparing the results in Fig.7 to those in Fig.6, the fatigue limit of the low hardness steels shown Fig.6 only depends on yield stress but that of high hardness steels in Fig.7 depends not only on yield stress but also on strain hardening coefficient and exponent. This indicates that harder steels are more sensitive to defects than softer steels in the sense that the fatigue limit of softer steels is influenced by only yield stress but that of harder steels depends on the shape of stress-strain curve.

The threshold of stress intensity factor calculated by Eqs.(10) and (11) is shown in Fig.8.  $\Delta K_{th}$  significantly increases with increasing  $\sigma_y$  but slightly increases with increasing  $A$ . On the other hand,  $\Delta K_{th}$  decreases with increasing  $n$ .  $\Delta K_{th}$  for the defect near specimen surface is larger than that for inside defect. These figures show that the most influential material constant on  $\Delta K_{th}$  is yield stress. That indicates that yield stress most contributes to the energy absorption due to crack extension.

## Conclusions

- (1) The Vickers hardness of the eight materials obtained from finite element analysis agreed to the

experimental results within 10% difference.

- (2) An equation to predict Vickers hardness was proposed as a function of yield stress ( $\sigma_y$ ), strain hardening coefficient ( $A$ ) and exponent ( $n$ ),

$$HV = \alpha A + \beta$$

$$\alpha = 4.499n^2 - 5.886n + (-1.810 \times 10^{-4}A + 2.525)$$

$$\beta = 2.701\sigma_y + 123$$

- (3) The fatigue limit of soft materials only increased with the increase of yield stress but it did not depend on strain hardening coefficient and exponent. The fatigue limit of hard materials increased with the increase of yield stress and strain hardening coefficient but it slightly decreased with increasing strain hardening exponent. The threshold of stress intensity factor of hard materials increased with increasing yield stress and strain hardening coefficient but it decreased with increasing strain hardening exponent.

#### References

- [1] Taber, D., 1951, *The Hardness of Metals*, Clarendon Press, Oxford.
- [2] Yoshizawa, T., 1967, *Hardness Testing and Its Applications*, Shokado Pub.
- [3] Karl, E. R., Komvopoulos, K., and Bogy D.B., 1993, "Elastic-Plastic Finite Element Analysis of Repeated Indentation of Half-Space by Rigid Sphere", *Trans. ASME, Journal of Applied Mechanics*, vol.60, No.4, pp.829-841.
- [4] Talijat, B., Zacharia, T., and Kosel, F., 1998, "New Analytical Procedure to Determine Stress-Strain Curve From Spherical Indentation Data", *Int. J. Solids Structures*, Vol.35, No.33, pp.4411-4426.
- [5] H.F.Wang and H.Bangert, 1993, "Three dimensional finite element simulation of Vickers indentation on coated systems", *Mater. Sic. and Engng.*, A163, pp.43-50.
- [6] Murakami, K. and Matsuda, K., 1991, "Analysis of Vickers hardness by the finite element method", *Trans. Japan Society of Mechanical Eng.*, Vol.A57, No.539, pp.1665-1673.
- [7] Hamada, N., and Sakane, M., 1999, "FEM Analysis for Brinell Hardness—The Effect of Inelastic Material Constants on Brinell Hardness —", *Trans. Japan Society of Mechanical Eng.*, Vol.A63, No.630, pp.254-260.
- [8] Hamada, N., Sakane, M. and Ohnami, M., 1998, "FEM Analysis for Rockwell Hardness (2nd Report, Rockwell A scale)", *Trans. Japan Society of Mechanical Eng.*, Vol.A64, No.621, pp.1356-1362.
- [9] Hamada, N., Sakane, M. and Ohnami, M., 1994, "FEM Analysis for Rockwell Hardness", *Trans. Japan Society of Mechanical Eng.*, Vol.A60, No.579, pp.2645-2652.
- [10] Hirano, A., Sakane, M., and Hamada, N., 2002 "Relationship Between Rockwell C Hardness and", pp.179-184.
- [11] Murakami, Y., Kodama, S. and Konuma S. 1987, "Quantitative Evaluation of Effect of Nonmetallic inclusion on Fatigue Strength of High Strength Steel", *Trans. Japan Society of Mechanical Eng.*, Vol.A54, No.500, pp.688-695.